



Research article

Effects of different types of flame-retardant treatment on the flame performance of polyurethane/wood-flour composites

Beibei Wang^{a,c}, Xuanye Wang^{a,c}, Lijuan Zhao^{a,c}, Qiuhui Zhang^{a,c}, Guochao Yang^{a,c,**}, Daihui Zhang^{b,*}, Hongwu Guo^{a,c,***}^a Key Laboratory of Wood Material Science and Application (Beijing Forestry University), Ministry of Education, Beijing 100083, China^b Institute of Chemical Industry of Forest Products, Chinese Academy of Forestry, Nanjing, 210042, Jiangsu, China^c Beijing Key Laboratory of Wood Science and Engineering, Beijing Forestry University, Beijing 100083, China

ARTICLE INFO

Keywords:

Foamed polyurethane/wood flour composite
Smoke suppression
Thermal degradation
Flame retardant mechanism

ABSTRACT

To improve the flammability of foamed polyurethane/wood-flour composites (FWPC), ammonium polyphosphate (APP) was used as a flame retardant to modified FWPC. The effects of different flame treatment processes on flame performance, smoke suppression, thermal property, and surface micrographs of flame retardant FWPC were investigated. The results showed that FWPC with the addition or impregnation process both improved the combustion behaviors. Compared with the addition process, FWPC-impregnation (FWPC-I) had a lower total heat release (THR), lower peak heat release rate (PHRR), prolonged time to ignition (TTI), more residues, and better combustion safety. FWPC-I had the highest residual carbon rate reaching 39.98%. A flame-retardant layer containing the P–O group was formed in the residual carbon of FWPC-I. Although APP had negative effects on the physical properties of FWPC, it was an effective flame-retardant ability for foamed polyurethane/wood-flour composites.

1. Introduction

Wood-plastic composites (WPC) have been widely used in commercial markets for many fields, such as automobile (interior panels, package trays, etc.) and construction (stairs, handrails, etc.) fields [1–3]. WPC products have been produced from different types of natural fiber resources and virgin thermoplastics including polyethylene [4], polypropylene [5], polyvinyl chloride [6], poly (lactic acid) [7]. Among them, polyurethane (PU) foam has been widely used in many fields due to its excellent properties [8,9]. In combination with wood processing residues (wood flour, wood fiber) and other wastes as blends, porous foamed polyurethane-based WPC can be prepared [10]. The physical and mechanical properties of WPC based on PU and wood flour (FWPC) have been previously investigated, and it proved that FWPC was a promising and sustainable green material. These composites have several advantages, including low density, high dimensional stability during a lifetime, high relative strength, and stiffness. The effective utilization of waste by FWPC also reduces carbon emissions and promotes the emission reduction of greenhouse gases.

* Corresponding author.

** Corresponding author. Key Laboratory of Wood Material Science and Application (Beijing Forestry University), Ministry of Education, Beijing 100083, China.

*** Corresponding author. Key Laboratory of Wood Material Science and Application (Beijing Forestry University), Ministry of Education, Beijing 100083, China.

E-mail addresses: yangguochao@bjfu.edu.cn (G. Yang), daihui.zhang@mail.mcgill.ca (D. Zhang), guohongwu305@bjfu.edu.cn (H. Guo).<https://doi.org/10.1016/j.heliyon.2023.e15825>

Received 23 February 2023; Received in revised form 17 April 2023; Accepted 24 April 2023

Available online 27 April 2023

2405-8440/© 2023 The Authors. Published by Elsevier Ltd. This is an open access article under the CC BY-NC-ND license (<http://creativecommons.org/licenses/by-nc-nd/4.0/>).

Although FWPC has been widely investigated, one serious drawback is its low ignition point and its flammability [11,12]. Moreover, the weak interfacial compatibility between wood flour and PU was another concern [13]. Besides, its high flammability restricts its applications in various fields such as high-security levels or folk house [14]. Therefore, the improvement of flame retardant FWPC is increasingly important and many efforts have been devoted to it. Xu et al. found that nanos and phosphorus flame retardants could reduce flammable gas release rate and form a highly protective char layer [15]. El-Fattah et al. proposed that organo-nano clay could improve flame retardancy properties [16]. Toshikazu et al. confirmed that wood flour and ammonium polyphosphate (APP) had synergy effects which can reduce the addition of APP [17]. Zhang et al. considered that silica had a flame-retardant synergistic effect with APP in wood-fiber/PP composite. [18]. Thus, a significant development has been made in this field.

Previously, various flame retardants for polymers and composites have been developed, and many of these are suitable for fiber-based composites [19]. The most effective method to enhance flame retardancy of WPC is the incorporation of flame retardants during the compounding process. APP is an effective intumescent fire retardant for several kinds of polymer-based materials. Its efficiency is generally attributed to the increase in char formation through a condensed phase reaction. Gracia et al. found that the addition of flame retardants caused the polyethylene-based composites to self-extinguish when APP or aluminum hydroxide were applied [19]. Douglas et al. found that the cross-linked network between cellulose, POSS, and PLA proved better flame retardant, rheological, and mechanical properties than other intumescent formulations [20]. Consequently, APP is an efficient flame retardant to improve fire resistance. Unfortunately, there is few information available for the flame-retardant polyurethane/wood flour composites treated by APP, especially the research on flame retardant treatment process. More importantly, the effect of different flame-retardant treatment processes on the flame retardancy was barely systematically investigated.

In this study, the effect of flame-retardant processes on the properties of FWPC was evaluated. The mechanical properties, flame retardancy, smoke suppression, and thermal decomposition were studied based on compressive strength tests, cone calorimetry tests (CCT), and thermogravimetric analysis (TGA), respectively. To further investigate the mechanism of APP on FWPC, the surface morphologies of flame retardant FWPC were examined by scanning electron microscopy (SEM) and energy dispersive spectroscopy (EDS). Moreover, the mechanism has also been studied by FT-IR spectra analysis and 2D-IR spectra analysis. This study provides a comprehensive knowledge about the effect of flame retardant on the properties of wood-plastic composites.

2. Material and methods

2.1. Materials

Polyurethane (PU, main components including diphenylmethane diisocyanate and polyols) with foaming capacity up to 78 times was obtained from Guanneng Polyurethane Company, Shanghai. Wood-flour of poplar (WF, *Populus tomentosa* Carr.) with particle size between 10 and 60 mesh was kindly supplied by Xingda Wood Flour Company, Hebei. A silane coupling agent (KH550, γ -Aminopropyltriethoxysilane) was purchased from Jinan Guobang Chemical Company, Shandong. Ammonium polyphosphate (APP) with an average polymerization $n < 100$ was produced by Haichengxingye Technology Company, Shenzhen.

2.2. Preparation of FWPC

Addition process: Wood flour was oven-dried for 8 h at 105 °C until the weight stabilized. Then, KH550, and APP were added into PU and WF with constant weight percentage (as shown in Table 1). Each group of raw materials was mixed in a container. After that, the samples were put into a mold with a dimension of 100 × 100 × 10 mm³ (length × width × height) and foamed in the drying oven at 60 °C for 60 min. Finally, the samples were taken out and cut into regular blocks for different tests. The control sample was prepared with no APP addition.

Impregnation process: Oven-dried wood flour was soaked in 20 wt% APP solution for 24 h until the flame-retardant liquid was completely absorbed (wood powder mass: solution mass = 4:5), then WF-APP was oven-dried in an oven at 105 °C until the weight stabilized. KH550 was added into PU and WF-APP with constant weight percentage. The following steps were the same as the addition process.

2.3. Testing and characterization

2.3.1. Physical performance test

Moisture absorption performance and dimensional stability test was performed according to GB/T 17657-2013 *Test methods of evaluating the properties of wood-based panels and surface decorated wood-based panels*. The sample was cut to a size of 25 × 25 × 25 mm³,

Table 1
Formulation of FWPC.

Sample	Composition based on weight (wt.%)			
	Wood-flour	PU	KH550	APP
Control	40	60	3	0
FWPC-A	40	60	3	10 (solid)
FWPC-I	40(WF-APP)	60	3	10 (solution)

immersed it in the water tank for 24 h, wiped off the surface moisture before the measurement. Compression performance test refers to GB/T20467-2006 *Flexible cellular polymeric materials - Moulded and extruded sponge or expanded cellular rubber products - Compressibility test on finished parts*. The sample is cut to $50 \times 30 \times 20 \text{ mm}^3$, and strength test is carried out on the universal testing machine. The loading speed is 0.5 mm s^{-1} .

2.3.2. Analysis of flame retardancy

The limit oxygen index test (LOI) is carried out according to the standard of GB/T 2406-2009 determination of combustion behaviors by oxygen index for plastics, and the digital display oxygen index meter m606b (Qingdao Shanfang Instrument Co., Ltd., China) is used. The test sample size is $80 \times 10 \times 10 \text{ mm}^3$, and 15 test samples were used for each group. The flame retardancy were performed on the treated samples using a cone calorimeter instrument (Stanton Redcroft, UK) according to the standard of ISO 5660 standard procedures. Each sample ($100 \times 100 \times 10 \text{ mm}^3$) was wrapped in aluminum foil and exposed horizontally to 50 kW m^{-2} external heat flux. Three replicates were tested for each group. At least three tests were performed.

2.3.3. Thermal stability analysis

To investigate the effect of flame-retardant treatment processes on the thermal decomposition behaviors of FWPC, TGA analysis was conducted. All TGA tests were recorded on a Q50 TGA analyzer (TA Instruments, USA) at a linear heating rate of $10 \text{ }^\circ\text{C min}^{-1}$ under a nitrogen atmosphere. The temperature ranged from ambient temperature to $700 \text{ }^\circ\text{C}$. Before the test, each sample was grounded into powders and kept with 5 mg in an open platinum pan.

2.3.4. Functional group analysis

FT-IR spectra analysis: The samples were examined by Spectrum GX Fourier-transform infrared spectrometer (PerkinElmer, USA) equipped with a DTGS detector. Before the test, all samples were grounded into powders. Each spectrum was collected at a resolution of 4 cm^{-1} and a total accumulation of 32 scans over the range is $4000\text{--}400 \text{ cm}^{-1}$. 2D-IR spectra analysis: The samples were put into the portable programmable temperature controller (Model 50-886, Love Control) to obtain 2D-IR spectra, which were connected to the spectrometer. Each spectrum was obtained by treatment of the series of temperature-dependent dynamic spectra at an interval of $10 \text{ }^\circ\text{C}$ during varying temperatures from 50 to $120 \text{ }^\circ\text{C}$ in the range of $700\text{--}1800 \text{ cm}^{-1}$, with 2D-IR correlation analysis software programmed by the Department of Chemistry of Tsinghua University, Beijing, China.

2.3.5. Micro morphology and elemental analysis

Field emission scanning electron microscope (FE-SEM) test: JSM-6700F FE-SEM equipped with X-ray probe is used, and the element content and distribution on the surface of the sample are detected by energy dispersion spectrometer (EDS). During the test, the electronic acceleration voltage is 15 kV, and all samples are sprayed with gold before the test.

3. Results and discussions

3.1. Effect of flame-retardant treatment on combustion performance of FWPC

To explore the flammability of FWPC before and after flame retardant treatment, the ignition of the sample was tested under different oxygen concentrations, and the LOI of the sample was obtained [10]. The test results showed that the LOI of the samples without flame retardant treatment was only 18.7%, while the LOI of FWPC-A after flame-retardant treatment with the APP was significantly improved with the value of 27.3%. In addition, the FWPC-I after impregnation flame-retardant treatment had a better flame-retardant effect, and its LOI was 29.4%. The comparison indicated that the impregnated flame retardant treated wood powder had a better flame-retardant effect under the same amount of flame retardant.

Aiming to investigate the effect of the impregnation process and addition process on the flame retardancy of FWPC during combustion, CCT was performed first 500 s of combustion phase in this study. CCT is an authoritative technique used to characterize the fire performance of small samples of various materials in the condensed phase. The heat release parameters of FWPC were listed in Table 2. Among them: TTI - time to ignition, HRR - heat release rate, PHRR - peak heat release rate, THR - total heat release, EHC - effective heat of combustion. TTI is an important index for determining the flame performance of materials. Compared to the control sample, the TTI values of flame-retardant samples were remarked prolonged from Table 2, especially for the impregnation sample with a TTI extended to 13 s. The reason might be due to the flame retardant militating the materials before the initial burning [2]. A longer TTI must be significant for early escape and firefighting.

HRR and its peak PHRR are usually considered as the most effective and important parameters for reflecting the flame performance of materials [21]. Moreover, PHRR and THR are also important indicators. As shown in Table 2, the average HRR of FWPC-A/I

Table 2
Cone calorimetry data of control, FWPC-A, and FWPC-I

Sample	LOI/(%)	TTI/(s)	Average HRR	PHRR/(kW m^{-2})	THR/(MJ m^{-2})	Residue/(%)
Control	18.7	8	186.84	416.88	86.1	15.89
FWPC-A	27.3	9	167.17	379.51	84.3	19.03
FWPC-I	29.4	13	172.12	313.84	74.9	24.10

decreased by 10.24% and 7.88%, respectively, and PHRR reduced by 8.96% and 24.72%. The THR of flame retardant FWPC was elevated, which reduced to 2.09% and 13.01% compared with control, respectively. Fig. 1a and b are HRR and THR curves of all samples which had relatively obvious peaks, and the HRR of FWPC treated with APP was much lower than the control. The PHRR was attributed to the dehydration of wood flour catalyzed by APP with combustion [22]. With the accumulation of the char residue, the combustion rate was suppressed. At the end of combustion, FWPC-I had the highest carbon residue content, which was 34.07% and 21.16% higher than FWPC-A and control, respectively. The increase in carbon residue indicates a decrease in the impact of combustion on material strength. The HRR curve, as well as the peak, decreased in intensity treated with APP, and the THR of FWPC treated with APP (FWPC-A/I) was lower than the controls.

From Fig. 1c, the smoke production rate (SPR) of FWPC-A/I treated with APP was lower than the control. The addition of flame retardant caused the SPR to further reduce. However, at the same loading of APP, the SPR value with the addition process was the lowest, suggesting that the addition process had a better smoke suppression effect than the impregnation process. Compared with total smoke product (TSP) in Fig. 1d, FWPC with APP showed effective smoke suppression. APP can greatly accelerate the formation of a dense char layer. The char residue can efficiently prevent the heat and gas transfer between the flame zone and burning matrix, which retarded the smoke production of FWPC. It was especially effective in chemically removing certain volatile fuels, which were responsible for promoting the formation of smoke particulates and combustion of specimens [23]. Similar results can be obtained from the TSP. The impregnation process exhibited smoke suppression at the beginning of the fire while increasing TSR 41.27% after the whole combustion. As far as smoke toxicity was concerned, the addition process exhibited better smoke performance than the impregnation process. The above phenomenon was due to the flame-retardant effect of APP on FWPC through addition, and the reagent was mainly distributed in PU, which effectively reduced the combustion of PU and inhibited the generation of flue gas.

The heat release parameters indicated that the fire performance of FWPC was enhanced by APP. This was mainly attributed to the formation of the char layer by adding APP. Another reason was that APP can prevent the cracking of the char layer. As shown in Fig. 2a, the control sample burned more completely. Wrinkles and cracks were found on the char layer of the additional sample during combustion as shown in Fig. 2b. However, as shown in Fig. 2c, it was observed that fewer cracks and more dense char residue were formed with the impregnation process, in which the char layer prevented heat transfer and reduced the HRR. It could be concluded that the impregnation process was better than the addition process to improve the flame retardancy of FWPC.

The smoke performance of flame-retardant material is an important parameter for evaluating fire hazards. It can directly cause death by releasing toxic gases. Table 3 listed the smoke release parameters of FWPC.

To give an overall evaluation of fire safety of materials, the fire performance index (FPI), fire growth index (FIGRA), smoke generation rate (SMOGRA) can be deduced from the measured values of CCT. They were defined as the ratio of TTI to PHRR, the ratio of PHRR to the time to PHRR, and the ratio of peak SPR to the time to peak SPR, respectively [24]. The higher FPI and the lower FIGRA and SMOGRA indicate better flame-retardant ability of materials [25]. Table 3 showed the fire risk deduction index of FWPC. FPI increased and FIGRA decreased with APP treatment, which indicated APP efficiently promoted the fire safety of FWPC. FWPC-A treated with addition process reduced SMOGRA by 60.88%, while impregnated FWPC-I had no significant effect on SMOGRA. The reason was that during the process of adding flame retardant APP, it was mostly dispersed on the surface of the material to form a flame-retardant layer containing phosphoric acid, which effectively reduced the generation of smoke. The APP in FWPC-I was added

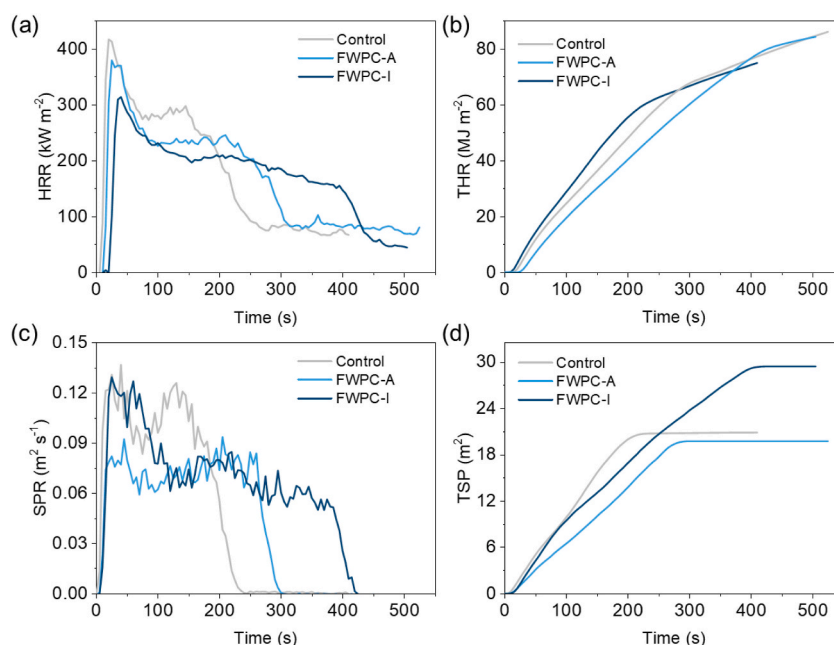


Fig. 1. (a) HRR, (b) THR, (c) SPR, and (d) TSP curves of FWPC.

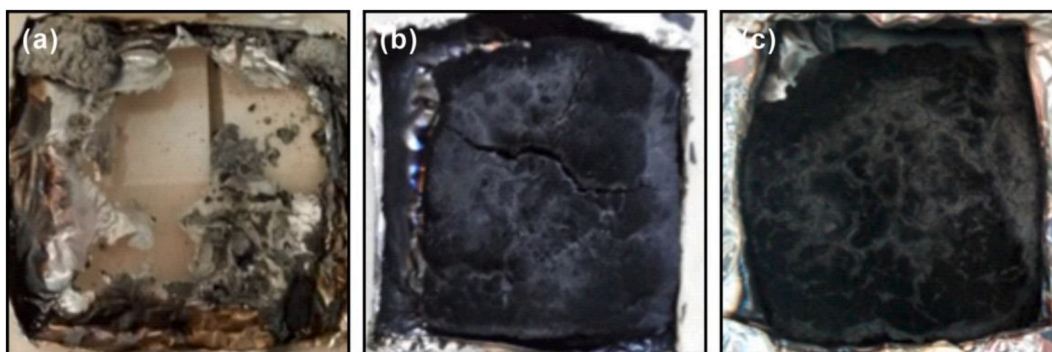


Fig. 2. Char formation of FWPC (a) Control, (b) FWPC-A, and (c) FWPC-I

Table 3
Fire risk deduction index of FWPC.

Sample	Control	FWPC-A	FWPC-I
FIGRA/(W S ⁻¹)	20.844	15.1804	7.846
FPI	0.01919	0.02372	0.04142
SMOGRA/(m ² s ⁻²)	0.00524	0.00205	0.00517

through impregnation process and had the characteristics of uniform dispersion, so the residual carbon of the surface flame retardant layer was easy to release into the air, resulting in high SMOGRA.

3.2. Test and analysis of thermal stability

TGA analysis is widely used to investigate the thermal stability of materials [10,26]. The thermal stability of materials is related to the release of decomposition and the formation of the carbon layer [27]. TGA and DTG curves of FWPC and main raw materials (APP, PU, and WF) on-air atmosphere were shown in Fig. 3. As shown in Fig. 3a, three main steps were observed. The first maximum weight reduction was due to the evaporation of water. The second decomposition peak took place at 162 °C which was assigned to the decomposition of short-chain APP with the release of ammonia and water, and then fragmented to volatile P₂O₅ at 549 °C in the third step [28]. The possible reaction of APP during combustion was shown in Fig. 4. The virgin PU showed one sharp degradation peak at 285 °C. PU foam was decomposed to produce isocyanate and alcohol which was ascribed to the weakest bond C–NH [29]. The maximum weight loss of around 350 °C was attributed to the decomposition of hemicellulose (200–300 °C), cellulose (300–400 °C), and lignin (200–900 °C) [30]. 17.3% char residuals were observed after thermal degradation analysis of WF. No synergistic effects were found for the combination of WF and PU used in this study.

Relevant node data are summarized in Table 4. During the heating process, the temperature point (T_{5%}) at which 5% mass was lost decreases with the addition of flame retardant. The decrease of T_{5%} may be caused by the addition of flame retardant. The flame-retardant APP would decompose at low temperature to produce ammonia and other components. It can absorb water at low temperature. As the combustion temperature increases, the absorbed water is released. With the further increase in temperature, the first thermogravimetric peak appeared near 280 °C. This stage was mainly caused by the thermal decomposition of PU. However, the peak value of FWPC-I decreased significantly, about 0.21% °C⁻¹ compared with control or FWPC-A. The peak difference was due to the

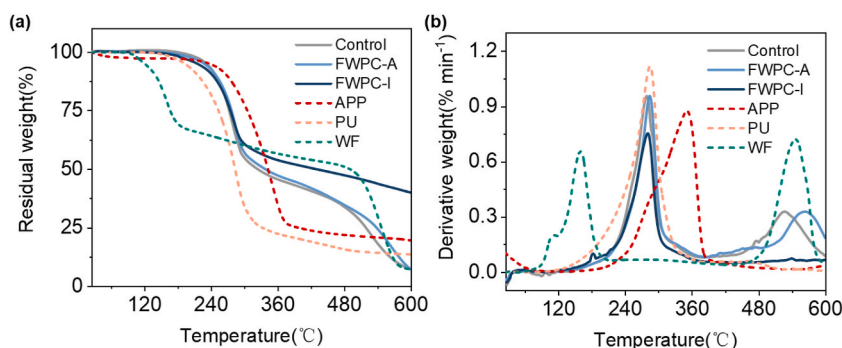


Fig. 3. (a) TGA and (b) DTG curves of control, FWPC-A, FWPC-I, APP, PU, and WF.

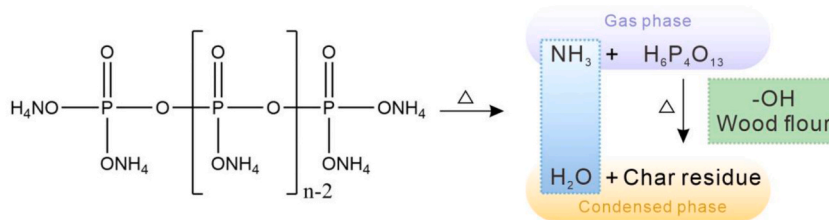


Fig. 4. Possible reaction of APP during the combustion.

Table 4

Fire risk deduction index of FWPC, APP, PU, and WF.

Sample	T ₅ (°C)	T _{max1} (°C)	PWD1 (% °C ⁻¹)	T _{max2} (°C)	PWD2 (% °C ⁻¹)	RC (%)
Control	231.81	278.18	0.95	528.14	0.33	7.12
FWPC-A	227.67	284.38	0.96	564.63	0.33	7.31
FWPC-I	215.11	280.83	0.75	–	–	39.98
APP	120.22	159.54	0.66	546.66	0.72	7.10
PU	192.49	284.92	1.12	–	–	13.52
WF	236.89	352.35	0.87	–	–	19.50

inhibition of PU decomposition by adding APP. Although the thermal temperature increased further, a second thermal weight loss peak appeared in both control and FWPC-A. The decomposition at this stage was mainly the decomposition of the wood fiber. The temperature of the thermal weight loss peak of FWPC-A increased by about 40 °C, which was due to the flame-retardant effect of the APP. However, the second thermogravimetric peak did not appear in FWPC-I. The main reason was that APP was fully immersed in wood fiber and inhibited the decomposition of the wood fiber. Therefore, the second obvious thermogravimetric peak did not appear (Fig. 3b). Among the residual carbon, FWPC-I had the highest residual carbon rate, and the effect of impregnation flame retardant treatment was obvious.

3.3. Functional group testing and analysis

To further investigate the flame-retardant mechanism of APP in FWPC, FTIR analysis was used to evaluate the thermal degradation behaviors of APP. FTIR spectra of the control, FWPC-A, and FWPC-I after CCT were shown in Fig. 5. The absorption band at 3300–2800 cm⁻¹ can be assigned to the –OH stretching in the two samples [31]. After adding APP, the absorption peak slightly moved to 3330 cm⁻¹. After the impregnation, the peak position of FMPC-I was shifted to 3343 cm⁻¹, which was assigned to the –NH stretching of primary amines and absorption peak of the free amino association group. A new absorption band appeared at 3206 cm⁻¹, which was attributed to the –NH stretching belonging to APP. Moreover, the characteristic peak of –NH was sharper than –OH. The control FWPC in the region of 2500–500 cm⁻¹ could be characterized by absorption peaks at 1726, 1664, 1596, and 1510 cm⁻¹ (C=C stretching

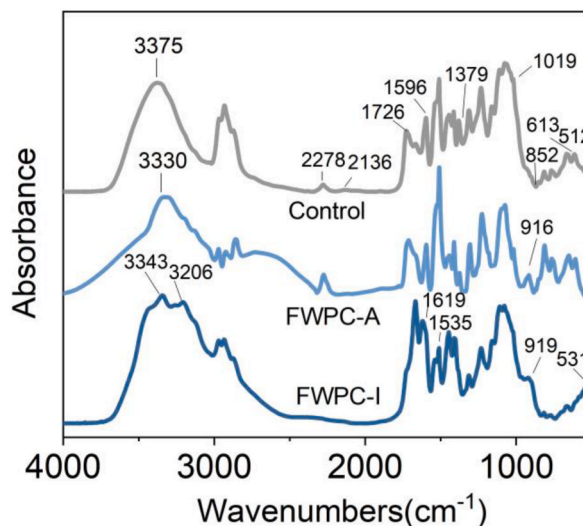


Fig. 5. FTIR analysis of control, FWPC-A, and FWPC-I

vibration), 1444 cm^{-1} (-CH bending vibration), 1413 , 1379 , and 1312 cm^{-1} (C-N stretching vibration), 1232 , 1161 , 1108 , and 1072 cm^{-1} (C=O stretching vibration), 1019 cm^{-1} (Si-O asymmetric stretching vibration), 850 , 814 , 766 , 666 , and 613 cm^{-1} (C-Cl stretching vibration) [12,32,33]. The intensity of the $3000\text{--}2800\text{ cm}^{-1}$ band decreased with the addition of APP. In FWPCs, the main component of PU, diphenylmethane diisocyanate, reacts with the free amino group in ammonium polyphosphate, resulting in the weakening of the characteristic peaks of methyl and methylene. For flame retardant FWPC, more changes occurred in the band of $1726\text{--}500\text{ cm}^{-1}$. It can be characterized by absorption peaks at 1535 cm^{-1} (N-H and C=O stretching owing to APP), the peaks at 2278 , 2136 , and 1726 cm^{-1} were weakened. A new peak at 919 cm^{-1} was the P-O stretching of APP [34].

2D-IR spectra usually enhanced the spectral resolution [12,34]. More peaks can be found and differences between the control and flame retardant FWPC were more significant using 2D-IR spectra [35–38]. Fig. 6 was 2D-IR spectra of the control and FWPC with the addition process. Changes in control FWPC were obvious in comparison with flame retardant FWPC. TGA analysis proved that flame retardant FWPC had high thermal stability, while FWPC was more sensitive to temperature disturbance than flame retardant FWPC during $50\text{--}120\text{ }^{\circ}\text{C}$.

In the 2D-IR spectra of the control sample, there were three strong auto peaks at about 725 cm^{-1} (assigned to the C-H bond bending vibration), 1200 cm^{-1} (assigned to the C-O bond stretching vibration), and 1400 cm^{-1} (assigned to the C-N bond stretching vibration), respectively. It meant that three peaks corresponding to the groups would change with the healing process, and it was sensitive to temperature disturbance. While in flame retardant FWPC, the peaks disappeared in the corresponding position (Fig. 6a). The position and intensity of peaks between 1600 and 1650 cm^{-1} were enhanced and moved to the right. This phenomenon revealed that the process of flame retardant was indeed helpful to reduce some of the chemical reactions to the heat-sensitive functional groups. In addition, two strong auto peaks also appeared at about 1100 and 1150 cm^{-1} which were assigned to components of APP, and several cross-peaks were also recorded in the region of $900\text{--}1100\text{ cm}^{-1}$. The presence of these absorption bands demonstrates the presence of new structures in FWPC-I (Fig. 6b). The flame-retardant APP may react with excess diphenyl methane diisocyanate and polyols in FWPC during the impregnation.

3.4. Micromorphology and element content analysis

Cross/top-sectional SEM images of FWPCs, and the corresponding energy-dispersive X-ray spectrometry (EDX) elemental mapping of Fe/TMS/PU/PA-10 before and after combustion are shown in Fig. 7. The preparation of flame retardant FWPC after impregnation did not damage the internal foaming structure. All of the FWPCs showed rich pore capsule structures (Figs. 7 a-1, b-1, c-1). After combustion, the pore capsule structure of Control was damaged and collapsed, resulting in the shrinkage after combustion (Figs. 7 a-2). The foaming phenomenon of FWPC-A and FWPC-I after combustion was caused by the decomposition of flame retardant and the formation of an intumescent flame-retardant layer (Figs. 7 b-2, c-2). When analyzing the micromorphology of the end face of the residual carbon after FWPC-I combustion, the distribution of the characteristic elements N and P of the flame retardant on the surface of the residual carbon was detected. The results were shown in Fig. 7d. The micromorphology results showed that a large number of microbubbles were formed on the surface, and a large number of P elements were distributed on the surface, which was similar to some n elements. The above results revealed that the P-containing flame-retardant layer was formed under the action of flame retardant to delay the combustion of the internal matrix.

The moisture absorption and compression properties before and after flame retardant treatment were tested and analyzed, and the results were shown in Fig. 8. Different flame-retardant treatments also had different physical properties of FWPC. The hygroscopicity

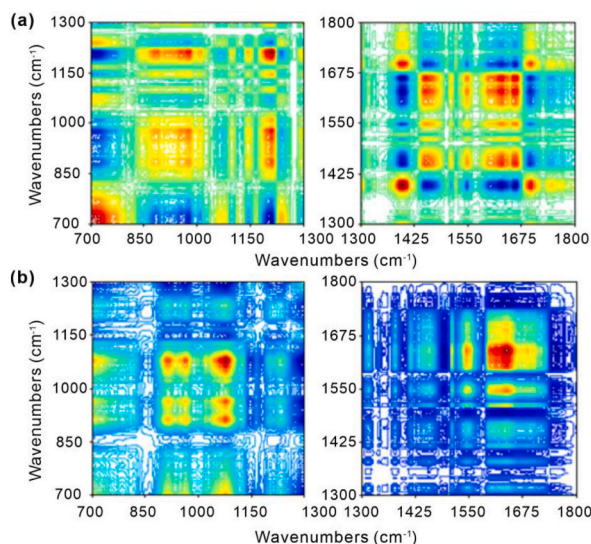


Fig. 6. 2D-IR analysis of (a) Control and (b) FWPC-I

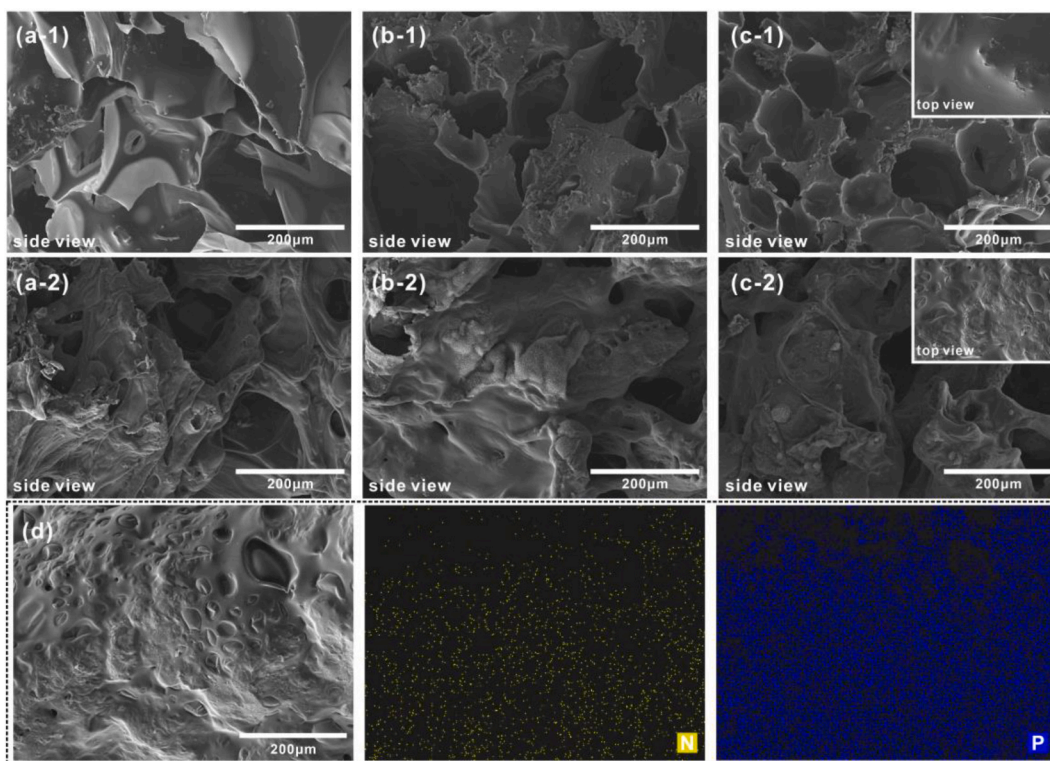


Fig. 7. FE-SEM of (a) Control, (b) FWPC-A, (c) FWPC-I, (–1) sample before combustion, (–2) after combustion, and corresponding EDX mapping of FWPC-I with the elemental distribution of N and P after CCT.

of FWPC-A after flame retardant treatment was significantly improved, while the hygroscopicity of FWPC-I after impregnation treatment was not significantly improved due to the less exposure of flame retardant relative to the way of addition, which was only 2.47% higher than that of control. At the same time, since the exposure of flame-retardant particles reduced the bonding strength between PU and wood fiber, the compression performance of FWPC-A was significantly reduced by about 26.2%. Nevertheless, the sample FWPC-I still maintained good compression resistance after impregnation, which was 2.89 MPa as compared to the 0.13 MPa of control.

After the flame-retardant treatment of FWPC, the solid-phase flame retardant property was formed on the surface of WPC while diluting combustible gas and O_2 by gas-phase flame retardant and solid-phase flame retardant [39,40]. The potential mechanism of flame-retardant action was shown in Fig. 9. Vapor phase flame retardant was mainly composed of ammonia released by APP decomposition and water vapor released by FWPC thermal decomposition. In addition, the strong acid phosphoric acid, pyrophosphoric acid, and metaphosphoric acid formed by the thermal decomposition of APP generated a glassy flame retardant on the surface of FWPC [41–43]. The formation of strong acid phosphorus-containing flame-retardant layer also promoted the dehydration of PU and wood fibers into carbon, forming a carbon layer, playing a role in isolating heat transfer and solid-phase flame retardant released by combustible materials.

4. Conclusion

Herein, the effects of different processes on thermal degradation, flammability, smoke suppression, and mechanical properties of wood plastic composites were systematically investigated. In contrast to the control, FWPC modified by APP showed better flame-retardant performance. The FWPC-I has the highest LOI was 29.4% and the lowest PHHR was about 313.84 kW m^{-2} . In the way of impregnation flame-retardant treatment, APP played a role on the surface and inside of FWPC-I through gas-phase and solid-phase flame retardance. The impregnation was an effective process to synthesize flame-retardant FWPC, since it showed less negative effect on the formation of porous structure and interfacial compatibility between wood and polymers. Also, the flame retardance could disperse evenly within the composites. This study demonstrates that the preparation process is also essential to improve the flame retardance of composites, and provides a new horizon to fabricate flame-retardant wood plastic composites.

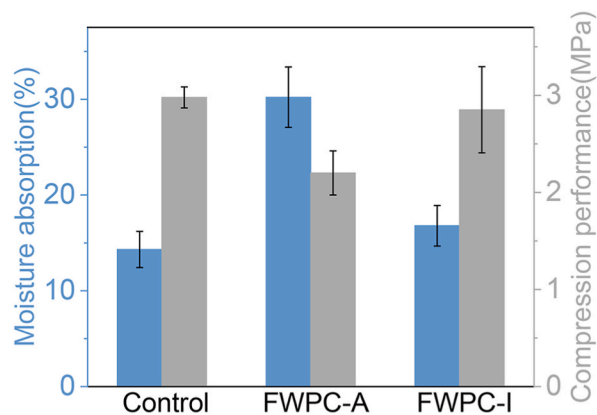


Fig. 8. Moisture absorption and compression properties of FWPC.

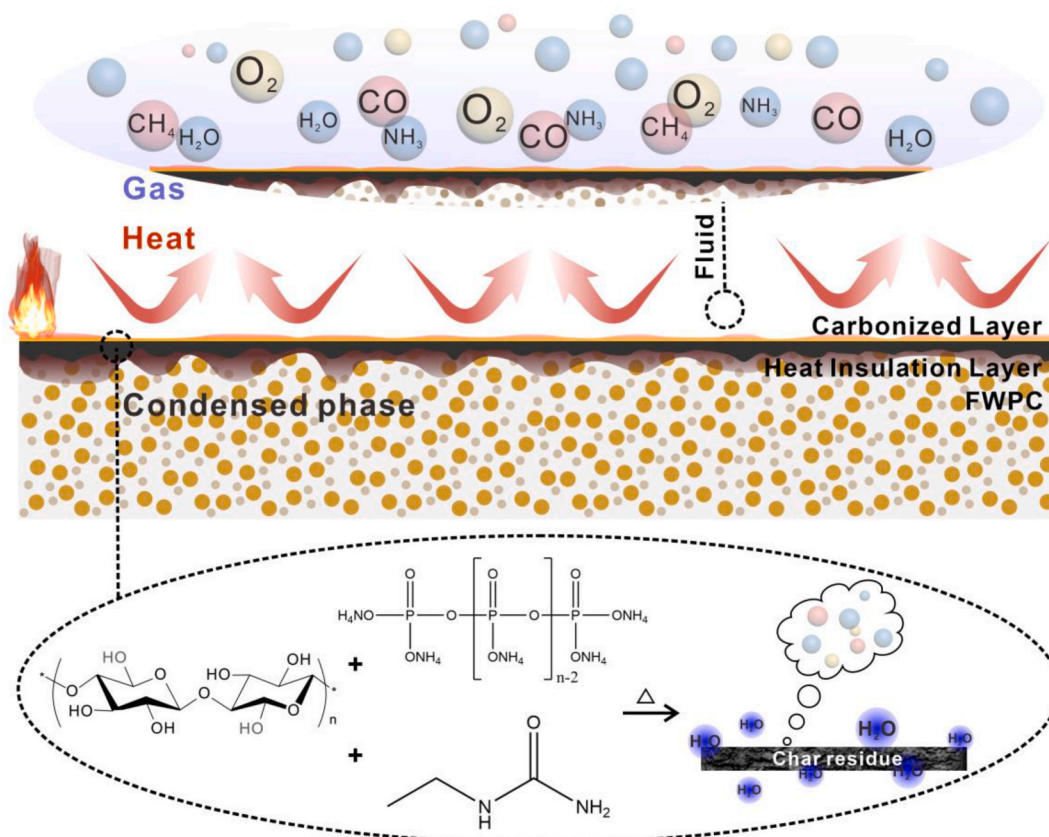


Fig. 9. Schematic illustration of the preparation and potential flame-retardant mechanism of FWPC-I

Declarations

Author contribution statement

Beibei Wang: Conceived and designed the experiments; Contributed reagents, materials, analysis tools or data; Wrote the paper.

Xuanye Wang, Lijuan Zhao: Performed the experiments.

Qihui Zhang, Guochao Yang: Analyzed and interpreted the data.

Daihui Zhang, Hongwu Guo: Conceived and designed the experiments; Contributed reagents, materials, analysis tools or data.

Funding statement

This work was supported by the Fundamental Research Funds for the Central Universities [BLX202134].

Data availability statement

Data will be made available on request.

Declaration of competing interest

The authors declare that they have no known competing financial interests or personal relationships that could have appeared to influence the work reported in this paper.

References

- [1] B. Kord, D.T. Haratbar, Influence of fiber surface treatment on the physical and mechanical properties of wood flour-reinforced polypropylene bionanocomposites, *J. Thermoplast. Compos. Mater.* 29 (2016) 979–992.
- [2] Suzuki Murayama, Kobori Kojima, Ogoe Ito, Okamoto, The effects of different types of maleic anhydride-modified polypropylene on the physical and mechanical properties of polypropylene-based wood/plastic composites, *J. Wood Chem. Technol.* 38 (2018) 224–232.
- [3] T. Lopez-Anido, Water absorption of wood polypropylene composite sheet piles and its influence on mechanical properties, *Construct. Build. Mater.* 25 (2011) 3977–3988.
- [4] A.K. Bledzki, M. Letman-Sakiewicz, M. Murr, Influence of static and cyclic climate condition on bending properties of wood plastic composites (WPC), *Express Polym. Lett.* 4 (2010) 364–372.
- [5] B. Gang, C. Guo, L. Li, Synergistic effect of intumescent flame retardant and expandable graphite on mechanical and flame-retardant properties of wood flour-polypropylene composites, *Construct. Build. Mater.* 50 (2014) 148–153.
- [6] O. Faruk, Matuana, Lm, Reinforcement of rigid PVC/wood-flour composites with multi-walled carbon nanotubes, *J. Vinyl Addit. Technol.* 14 (2008) 60–64.
- [7] A.P. Mathew, K. Oksman, M. Sain, Mechanical properties of biodegradable composites from poly lactic acid (PLA) and microcrystalline cellulose (MCC), *J. Appl. Polym. Sci.* 97 (2005) 2014–2025.
- [8] W. Xi, L. Qian, Y. Chen, J. Wang, X. Liu, Addition flame-retardant behaviors of expandable graphite and [bis(2-hydroxyethyl)amino]-methyl-phosphonic acid dimethyl ester in rigid polyurethane foams, *Polym. Degrad. Stabil.* 122 (2015) 36–43.
- [9] W. Xi, L. Qian, L. Li, Flame retardant behavior of ternary synergistic systems in rigid polyurethane foams, *Polymers* 11 (2019) 207.
- [10] B. Wang, X. Wang, Y. Liu, Q. Zhang, G. Yang, D. Zhang, H. Guo, Phytic acid-Fe chelate cold-pressed self-forming high-strength polyurethane/marigold straw composite with flame retardance and smoke suppression, *Polym. Degrad. Stabil.* 208 (2023), 110269.
- [11] K. Wang, S. Gao, C. Lai, Y. Xie, Y. Sun, J. Wang, C. Wang, Q. Yong, F. Chu, D. Zhang, Upgrading wood biorefinery: an integration strategy for sugar production and reactive lignin preparation, *Ind. Crop. Prod.* 187 (2022), 115366.
- [12] X. Xu, K. Wang, Y. Zhou, C. Lai, D. Zhang, C. Xia, A. Pugazhendhi, Comparison of organosolv pretreatment of masson pine with different solvents in promoting delignification and enzymatic hydrolysis efficiency, *Fuel* 338 (2023), 127361.
- [13] E. Moritzer, M. Hopp, Bonding of wood-plastic composites (WPC)—material and surface modification for special applications, *Welding in the World, Le Soudage Dans Le Monde* 61 (2017) 1029–1038.
- [14] Mingzhu, Pan, A novel fire retardant affects fire performance and mechanical properties of wood flour-high density polyethylene composites, *Bioresources* 7 (2012) 1760–1770.
- [15] W. Xu, G. Wang, X. Zheng, Research on highly flame-retardant rigid PU foams by combination of nanostructured additives and phosphorus flame retardants, *Polym. Degrad. Stabil.* 111 (2015) 142–150.
- [16] E.F. A, A.M.E.S. B, M.M.D. A, B. ES, Studying the effect of organo-modified nanoclay loading on the thermal stability, flame retardant, anti-corrosive and mechanical properties of polyurethane nanocomposite for surface coating, *Prog. Org. Coating* 89 (2015) 212–219.
- [17] T. Umemura, Y. Arai, S. Nakamura, Y. Tomita, T. Tanaka, Synergy effects of wood flour and fire retardants in flammability of wood-plastic composites, *Energy Proc.* 56 (2014) 48–56.
- [18] Z.X.B.X. Zhang, Kang Xin, C.K. Kim, Jk, Effect of flame retardants on mechanical properties, flammability and foamability of PP/wood-fiber composites, *Compos. B Eng.* 43 (2012) 150–158.
- [19] Hidalgo Garcia, Garmendia, G. Ca, Wood-plastics composites with better fire retardancy and durability performance, *Compos. Part A-Appl. Sci. Manuf.* 40 (2009) 1772–1776.
- [20] D.M. Fox, M. Novy, K. Brown, M. Zammarano, R.H. Harris, M. Murariu, E.D. McCarthy, J.E. Seppala, J.W. Gilman, Flame retarded poly(lactic acid) using POSS-modified cellulose. 2. Effects of intumescent flame retardant formulations on polymer degradation and composite physical properties, *Polym. Degrad. Stabil.* 106 (2014) 54–62.
- [21] W. Chen, H. Li, L. Li, X. Wang, Reinforcing condensed phase flame retardancy through surface migration of Brucite@Zinc borate-incorporated systems, *ACS Omega* 5 (2020) 28186–28195.
- [22] Y. Ren, Y. Wang, L. Wang, T. Liu, Evaluation of intumescent fire retardants and synergistic agents for use in wood flour/recycled polypropylene composites, *Construct. Build. Mater.* 76 (2015) 273–278.
- [23] W. Wang, S. Zhang, F. Wang, Y. Yan, J. Li, W. Zhang, Effect of microencapsulated ammonium polyphosphate on flame retardancy and mechanical properties of wood flour/polypropylene composites, *Polym. Compos.* 37 (2016) 666–673.
- [24] X. Chen, L. Liu, J. Zhuo, C. Jiao, Influence of iron oxide Brown on smoke-suppression properties and combustion behavior of intumescent flame-retardant epoxy composites, *Adv. Polym. Technol.* 34 (2015) 625–633.
- [25] X. Zhang, O. Alloul, Q. He, J. Zhu, Verde, M. J, Strengthened magnetic epoxy nanocomposites with protruding nanoparticles on the graphene nanosheets, *Poly. Int. J. Sci. Techn. Poly.* 54 (2013) 3594–3604.
- [26] X. Qian, S. Lei, H. Yuan, R. Yuen, Preparation and thermal properties of novel organic/inorganic network hybrid materials containing silicon and phosphate, *J. Polym. Res.* 19 (2012) 9890.
- [27] D. Jiang, H. Xu, S. Lv, D. Jiang, S. Cui, S. Sun, X. Song, S. He, J. Zhang, Properties of flame-retardant leaf fiber cement-based composites at high temperatures, *Heliyon* 8 (2022), e12175.
- [28] J. Li, X. Zeng, D. Kong, H. Xu, L. Zhang, Y. Zhong, X. Sui, Z. Mao, Synergistic effects of a novel silicon-containing triazine charring agent on the flame-retardant properties of poly(ethylene terephthalate)/hexakis (4-phenoxy)cyclotriphosphazene composites, *Polym. Compos.* 39 (2018) 858–868.
- [29] Y. Rong, W. Hu, X. Liang, S. Yan, J. Li, Synthesis, mechanical properties and fire behaviors of rigid polyurethane foam with a reactive flame retardant containing phosphazene and phosphate, *Polym. Degrad. Stabil.* 122 (2015) 102–109.
- [30] L.H. Pham, D.N. Hai, J. Kim, D.Q. Hoang, Thermal properties and fire retardancy of polypropylene/wood flour composites containing eco-friendly flame retardants, *Fibers Polym.* 20 (2019) 2383–2389.

- [31] T. Lu, J. Zhang, Y. Wei, P. Shen, Effects of ferric oxide on the microbial community and functioning during anaerobic digestion of swine manure, *Bioresour. Technol.* 287 (2019), 121393.
- [32] B. Wang, Y. Li, W. Zhang, J. Sun, J. Zhao, Y. Xu, Y. Liu, H. Guo, D. Zhang, Ultrathin cellulose nanofiber/carbon nanotube/Ti3C2Tx film for electromagnetic interference shielding and energy storage, *Carbohydr. Polym.* 286 (2022), 119302.
- [33] X. Xu, D. Zhang, K. Wang, Y. Jia, C. Yang, B. Shen, C. Lai, Q. Yong, In-situ lignin modification with polyethylene glycol-epoxides to boost enzymatic hydrolysis of combined-pretreated masson pine, *Bioresour. Technol.* 344 (2022), 126315.
- [34] P. Zhao, C. Guo, LipingLi, Exploring the effect of melamine pyrophosphate and aluminum hypophosphite on flame retardant wood flour/polypropylene composites, *Construct. Build. Mater.* 170 (2018).
- [35] I. Noda, Advances in two-dimensional correlation spectroscopy, *Vib. Spectrosc.* 36 (2004) 143–165.
- [36] I. Noda, *Advances in Two-Dimensional Correlation Spectroscopy, 2DCOS*, 2018.
- [37] B. Huang, C. Fang, L. Chen, X. Wang, X. Ma, H. Liu, X. Zhang, F. Sun, B. Fei, A novel ecological, highly-utilizable manufacturing technology for standard bamboo units and its deformation laws, *Ind. Crop. Prod.* 183 (2022), 115008.
- [38] Z. Liu, H. Li, X. Gao, X. Guo, S. Wang, Y. Fang, G. Song, Rational highly dispersed ruthenium for reductive catalytic fractionation of lignocellulose, *Nat. Commun.* 13 (2022).
- [39] C. Deng, J. Zhao, C.L. Deng, Q. Lv, L. Chen, Y.Z. Wang, Effect of two types of iron MMTs on the flame retardation of LDPE composite, *Polym. Degrad. Stabil.* 103 (2014) 1–10.
- [40] F. Laoutid, L. Bonnaud, M. Alexandre, J.M. Lopez-Cuesta, P. Dubois, New prospects in flame retardant polymer materials: from fundamentals to nanocomposites, *Mater. Sci. Eng. R Rep.* 63 (2009) 100–125.
- [41] J. Luo, C. Li, X. Li, J. Luo, Q. Gao, J. Li, A new soybean meal-based bioadhesive enhanced with 5,5-dimethyl hydantoin polyepoxide for the improved water resistance of plywood, *RSC Adv.* 5 (2015) 62957–62965.
- [42] J.B. Chen, S.Q. Sun, Q. Zhou, Infrared microspectroscopic identification of marker ingredients in the finished herbal products based on the inherent heterogeneity of natural medicines, *Anal. Bioanal. Chem.* 406 (2014) 4513–4525.
- [43] H. Wang, X. Shi, Y. Xie, S. Gao, Y. Dai, C. Lai, D. Zhang, C. Wang, Z. Guo, F. Chu, A furan-containing biomimetic multiphase structure for strong and supertough sustainable adhesives, *Cell Rep. Phys. Sci.* (2023), 101374.